Mass Transfer in Horizontally Moving Stable Aqueous Foams

EUGENE Y. WEISSMAN and SEYMOUR CALVERT

Case Institute of Technology, Cleveland, Ohio

An efficient gas absorption device has been developed based on a stable aqueous foam moving in a horizontal duct, with a gas-liquid interaction that causes only negligible pressure drops.

The study of a liquid-phase and a mostly gas-phase-controlled system has indicated that their mass transfer performance can be predicted. This is based on hydrodynamic data for flowing foams, obtained in a preliminary study published elsewhere.

The influence of geometry, foaming solution properties, and surfactant-caused interfacial resistance are included in the analysis.

Foaming systems have lately been receiving increased attention for heat and mass transfer applications owing to the large interfacial areas they offer from relatively low amounts of liquid.

Work on gas-bubble columns was reported as early as 1950 by Shulman and Molstad (*40*). Additional work of both practical and theoretical interest has since been published (*11, 15, 16,* 39).

The use of foam rather than bubble assemblies is apparently reported only since 1955, when Helsby and Birt (13) found greater efficiencies of absorption of carbon dioxide in foam columns than in packed columns. Metzner and Brown (*21*) published their findings in the area of mass transfer in foam columns in 1956, stressing the disadvantage of high pressure drops and applicability limited to unconventional situations. Since then, the field has become more and more active (*5, 8, 10, 17* to *20, 22* to *28, 31* to *36, 41* to *43, 45*) but the investigations were limited to the technique of countercurrent contacting on sieve plates with correspondingly large operating pressure drops. This is particularly the case for highly intensified gas-liquid contacting, that is high flow rates and pure liquids (no surfactants added). Such dynamically stable foams collapse below a critical gas flow rate.

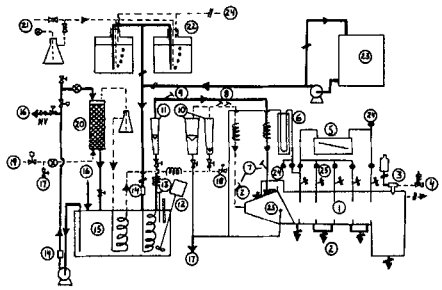

Fig. 1. Diagram of the experimental installation. (1) The foam-apparatus; (2) drain and liquid sampling points; (3) antifoam spray assembly; (4) 100 lb. per sq. in. g. air source; (5) inclined-tube manometer filled with specific gravity 0.827 red oil; (6) U-tube manometer (two of them; one filled with water, the other one with mercury); (7) thermometer with 0.2°C. subdivisions; (8) Wet- and dry-bulb thermometer; (9) dial thermometer; (10) gas rotameter; (11) liquid rotameter; (12) stirrer assembly; (13) Fenwal thermo-switch and thermometer with 0.1°C. subdivisions; (14) strainer; (15) constant-temperature bath; (16) from or to jacket of Ross-Miles apparatus; (17) line drain; (18) regulating vent; (19) blower air supply; (20) air humidifier; (21) atmospheric air and carbon-dioxide supply; (2) feed bottles; (23) solution preparation tank; (24) vent; (25) connections for pressure measurement and gas sampling.

Symbols: globe valve; gate valve; NV needle valve; ⊗ check valve; ⊗ toggle valve; screw clamp or quick-acting pinch-cock; solenoid valve; heating tape; centrifugal pump; ——— liquid line; - - - - gas line, ——— pressure measurement line.

Some different approaches have also been published. Workman (*48*) reported on sieve plate arrangements with and without egg crate supports for the froths that were formed. Ungemach (*43*) published a brief note on an inclined baffled tube arrangement, and an application to heat exchange (*29*) is under study.

This paper treats the gas desorption from a moving aqueous foam. In the present case, however, the foam has been generated by pretreatment of the liquid phase (water) with a small amount of a surface-active agent (saponin)* prior to contacting with a gas phase. Thus, a suitable surface activity has been induced in the liquid, and high rates of momentum transfer are no longer necessary for the obtention of a stable foam.

APPARATUS AND PROCEDURE

The desorption of carbon dioxide from water (liquid-phase controlled system) and of ammonia from water (almost gas-phase controlled) were studied under identical sets of operating conditions and geometries. The stripping gas was air [containing 350 p.p.m. carbon dioxide (*46*)]. It also made the solution foam and was presaturated with water at the run temperature (30°C.).

* Saponin is an extract of naturally occurring glucosides, nonionic in character, and known to produce very stable slow-draining foams. An 0.2% concentration by weight was found to be the minimum amount permitting good operation of the foam apparatus over a wide range of gas and liquid flow rates while not affecting the equilibrium relationships carbon dioxide-water and ammonia-water (*46*).

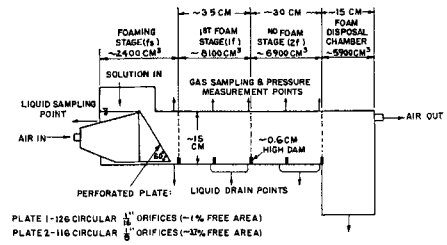

Fig. 2. Schematic representation of foam apparatus showing the division by stages.

Eugene Y. Weissman is with the General Electric Company, Lynn River Works, Lynn, Massachusetts. Seymour Calvert is at The Pennsylvania State University, University Park, Pennsylvania.

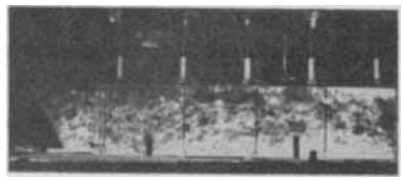

Fig. 3. Apparatus in operation (⅛-in. plate holes, 5 std. cu. ft./min. air, 1,050 cc./min. liquid).

Apart from offering the advantage of better control of the experimental conditions, desorption also yields truer measurements of the diffusional rates of mass transfer. Thus, it was found (*46*) that both carbon dioxide and ammonia increase the surface tension of the solution when absorbed in it. As a result, the apparent measured rate of absorption would also include the contribution of convection currents tending to restore the decreasing surface tension gradient in the liquid, in a direction perpendicular to the interface (*1, 2, 12*) with the lowest surface tension at the interface. Conversely, during desorption this surface-tension equilibrium is not disturbed.

The complete experimental installation is described schematically in Figure 1. The foam apparatus and its various stages, defined and investigated separately during this work, is represented in Figure 2, while Figure 3 is a photograph of the apparatus in operation.

With this setup the only pressure loss occurred at the perforated plate. No measurable pressure drop could be detected, owing to the moving foam column, over the entire practical range of gas and liquid flow rates. The pressure drops throughout the plate are minor (maximum 5 cm. water) because the apparatus must operate at low gas flow rates (in this case, up to 30 cm./sec.) for efficient foam operation.

In a typical run, after the gas stream had been brought to the desired temperature and humidity and the foaming solution had been readied in the constant-head vessels, the two streams were metered into the apparatus at the desired flow rate. The measurements were started only after the liquid stream was at the gas temperature. By that time at least fifteen apparatus volumes of foam had passed through the duct.

Flow rates, pressures, and temperatures were recorded and liquid and gas samples collected. Each apparatus stage was considered individually. Gas sampling was subsequently discontinued as it did not yield average concentrations representative of the foam stage under study. The liquid samples did so, since they were the result of the draining of the totality of foam cell lamellae in a given foam column section (stage).

In addition to various combinations of gas and liquid flow rates and plate geometries, the influence of the following physical parameters (in carbon dioxide solutions) was also studied:

1. Surface tension (at constant bulk viscosity and specific gravity), by varying the saponin content from 0.10 to 0.75% by weight, which is 0.25% above the critical micelle concentration (*46*). The corresponding surface tension change was from 44.5 to 36.6 dynes/cm.

2. Bulk viscosity (at constant surface tension and specific gravity), by adding to a 0.2% saponin solution from 0.1 to 0.2% by weight of Natrosol 250,* giving a corresponding viscosity change from 0.8 centipoises for 0% Natrosol to 5.5 centipoises for 0.2% Natrosol solutions.

Carbon dioxide in the saponin containing liquid samples was determined by first stripping it out with carbon dioxide-free air and then absorbing in Ascarite and Anhydrone.

Pure water-carbon dioxide solutions were also analyzed by excess treatment with barium hydroxide in the presence of barium chloride and backtitration with hydrochloric acid in the presence of phenol-phthalein as an indicator. An alternative method, also used, was the measurement of electric conductivity of the aqueous sample.

Ammonia liquid samples were titrated with hydrochloric acid in the presence of a mixed indicator (methyl red + methylene blue) with a correction factor obtained from blank saponin containing samples.

* Natrosol 250 is a hydroxyethylated cellulose, nonionic in character.

Surface tensions were determined with the Du Nouy ring method (*4*), bulk viscosities by Ubbelohde viscometry, foaminess and foam stability by the Ross-Miles method (*3, 37, 38*), and specific gravity by hydrometry with temperature correction.

On separate runs the following foam characteristics were also determined: interfacial areas, by photography; fractional liquid hold ups, by a technique based on an instantaneous stopping of the gas and liquid flow rates after steady operating conditions had been attained, and measurement of the amount of liquid collected from the killed foam section in each stage.

A detailed description of the equipment and experimental procedure has been given elsewhere (*46*).

ESTIMATION OF THE RATES OF MASS TRANSFER

In essence, the foam results from crosscurrent contacting of a liquid phase with a gas phase. And even after it has been generated and moves along the duct, this crosscurrent interaction continues in the sense that the gas moves horizontally forward and liquid drains out of the foam lamellae, downward. In addition, a portion of the gas phase continues to exist as an independent phase even after the flowing foam has been generated. This portion channels through the moving foam column at a faster rate than the column itself. The channeling becomes more pronounced as the flow rates decrease towards their critical values below which no effective foam can be obtained.

The arbitrary division of the foam column into two stages (Figure 2) has a mechanistic justification. Thus the first foam stage is the active part, as indicated by its intense draining and marked contribution to the overall transfer process, and the second foam stage is already spent, passive from the same points of view (*46*).

An added clarification of the mechanisms occurring in the foam apparatus requires a further subdivision of the foaming stage into three zones:

1. The plate zone (p) where the downflowing layer of foaming solution is contacted by gas passing through the perforations. In general, high fractions of the incoming liquid drain out of this zone without apparently foaming at all.

2. The bubble formation zone (b), taken as a slice of the foaming stage parallel to the plate and of a thickness equal to the radius of an average bubble being formed (taken as equal to half the pitch). It is here that the bubbles form, grow, and coalesce into a stable foam.

3. The foam zone (f) which is similar in character to the foam stages that follow downstream. It represents the downstream end of the foaming stage.

The integrated rate expressions for mass transfer in a liquid-phase controlled system and in a gas-phase controlled system are, respectively:

$$N = \frac{\rho_L}{M_w} K_{LG} A (X - X^*) \qquad (1)$$

and

$$N = \frac{\rho_G}{M_A} K_{GG} A (Y^* - Y) \qquad (2)$$

The material balances yield

$$N = (\lambda_i)_{stage} (X_i - X_o) \text{ and } N = \bar{\gamma}(Y_o - Y_i) \quad (3, 4)$$

Both systems obey Henry's law in the range of concentrations and pressures under consideration and are sufficiently dilute to warrant the assumption of a straight operating line and of the following approximation for the overall number of transfer units:

$$N_{toL} = \int_{X_1}^{X_2} \frac{dX}{X - X^*} = \frac{X_2 - X_1}{(\overline{X - X^*})} \text{ and}$$

$$N_{toG} = \int_{Y_2}^{Y_1} \frac{dY}{Y^* - Y} = \frac{Y_1 - Y_2}{(\overline{Y^* - Y})} \qquad (5, 6)$$

Utilizing Pozin's simplified and yet sufficiently accurate expression for the magnitude of the average driving forces $(\overline{X - X^*})$ or $(\overline{Y^* - Y})$ in crosscurrent flow (*30*) and rearranging, one obtains

$$N_{toL} = \frac{\rho_L}{M_W} \frac{A\,K_{LC}}{(\lambda_t)_{\text{stage}}} = \frac{X_t - X_o}{\dfrac{X^*_t - X^*_o}{2} - \dfrac{X_o - X_t}{\ln\left(\dfrac{X_t^* - X_t}{X_t^* - X_o}\right)}} \qquad (7)$$

$$N_{toG} = \frac{\rho_G}{M_A} \frac{K_{GC}\,A}{\overline{\gamma}} = \frac{Y_o - Y_t}{\dfrac{Y_t^* - Y_o^*}{\ln\left(\dfrac{Y_t^* - Y_t}{Y_o^* - Y_t}\right)} - \dfrac{Y_t - Y_o}{2}} \qquad (8)$$

where the left-hand side of Equations (7) and (8) is used for the predictions and compared with the experimental right-hand side.

Equation (7) can be further simplified by noting that $X_t^* \approx 0$, $X_o^* \approx 0$, and one finally obtains

$$N_{toL} = \frac{\rho_L}{M_W} \frac{A\,K_{LC}}{(\lambda)_{\text{stage}}} \approx \ln\left(\frac{X_t}{X_o}\right) \approx N_{tL} \qquad (9)$$

The mass transfer coefficients have been evaluated by means of the penetration theory (*14*):

$$K_{LC} = \left(\frac{4D_L}{\pi}\right)^{0.5} \frac{1}{t^{0.5}} \qquad (10)$$

for carbon dioxide desorption, and

$$K_{GC} = \left(\frac{4D_G}{\pi}\right)^{0.5} \frac{1}{t^{0.5}} \qquad (11)$$

for Ammonia desorption.

The corresponding penetration times t have been derived based on the mechanisms of gas-liquid interaction as observed in the various postulated stages and zones of the apparatus. Space considerations preclude a detailed presentation of the analysis, already available elsewhere (*46*). The results are outlined below.

Peneration times t for various situations

Carbon dioxide desorption

Plate zone—see discussion below regarding N_{tf}.

Bubble formation zone—

$$t_b = \frac{\rho_L}{M_W} V_b \left(\frac{\mathcal{L}_f}{\overline{\lambda}_b}\right) \qquad (12)$$

Foam zone
First foam stage
Second foam stage

$$t = \frac{\rho_L}{M_W} S_B l' \left(\frac{\mathcal{L}}{\lambda_\Delta}\right) \qquad (13)$$

Ammonia desorption

Plate zone—

$$t_{p\sigma} = 2.96 \times 10^{-4} \pi \left(\frac{\mu_L M_W}{g\,\rho_L^2}\right)^{0.333} \frac{P}{T} \frac{N_h d_h^2}{(b \sin \phi)^{0.333}} \left(\frac{\lambda_t^{0.333}}{G_v}\right) \qquad (14)$$

Bubble formation zone—

$$t_b = 4.10 \times 10^{-4}\, pS \frac{P}{T} \left(\frac{1}{G_v}\right) \qquad (15)$$

Foam zone
First foam stage
Second foam stage

$$t = 8.20 \times 10^{-4}\, l'S \frac{P}{T} \left(\frac{1 - \mathcal{L}}{G_v}\right) \qquad (16)$$

Several adjustments, in the form of correction factors, are necessary before the prediction equations for N_t, the number of transfer units, can be used.

One of them, general to both the liquid and the gas-phase controlled systems, is due to the physico-chemical interfacial resistance to mass transfer caused by the surfactant (Saponin) molecules preferentially adsorbed at the interface. It has been shown (*9, 44, 46*) how the following expression is sufficiently accurate to be used as the appropriate correction factor:

$$\exp\left[-\frac{(\sigma - \sigma_S)\omega}{R'T}\right]$$

It is based on the fact that the chemical potentials of the solute (transferring component) at the interface and in the bulk of the solution (with or without surfactant) differ by the amount

$$\sigma\omega$$

A second correction factor, applicable only to the liquid-phase controlled system, is necessary in order to account for the finite thickness of the liquid foam films (*6*). It is defined as the ratio of the approach to equilibrium in a finite system, such as this, to that of a semi-infinite one (as for the penetration theory):

$$\frac{(M_t/M_\infty)_\phi}{(M_t/M_\infty)_\Sigma} \qquad (18)$$

In this case, whether one is dealing with a hollow sphere in the bubble formation zone or a plane sheet in the foam column between two adjacent foam cells, one obtains for the semi-infinite case

$$\left(\frac{M_t}{M_\infty}\right)_\Sigma = 2.257\left[\frac{D_L t}{(\delta')^2}\right] \qquad (19)$$

where

$$\delta' = 2\frac{\mathcal{L}}{a} \text{ (46, 47)} \qquad (20)$$

For the finite case the following solutions can be derived (6^{bis}):

For the bubble formation zone

$$\left(\frac{M_t}{M_\infty}\right)_\phi \approx 1 - \frac{384\,(a')^2}{\pi^2[48(a')^2 + (\delta'_f)^2]} \exp\left[-4\pi^2 \frac{D_L\, t_b}{(\delta'_f)^2}\right] \qquad (21)$$

where

$$a' = \frac{2.51}{a\mathcal{L}^{0.01}} \text{ (46, 47)} \qquad (22)$$

For the foam zone and stages

$$\left(\frac{M_t}{M_\infty}\right)_\phi \approx 1 - 0.811 \exp - \left[9.86 \frac{D_L t}{(\delta')^2}\right] \qquad (23)$$

Finally, the gas-phase controlled system, also requires a second correction factor which takes into account the gas-channeling effect. It is given by

$$\left(\frac{\overline{v}_H}{u_H}\right)^{0.5} \qquad (24)$$

where

$$\overline{v}_H = \frac{M_w}{\rho_L} \frac{\overline{\lambda}}{S\mathcal{L}} \qquad (25)$$

$$u_{\mathcal{H}} = \frac{1{,}218.8}{S}\,\frac{T}{P}\,\frac{G_v}{(1-\mathcal{L})} \tag{26}$$

This corrects accordingly the value of the mass transfer coefficient predicted by means of a penetration time based on $u_{\mathcal{H}}$ (see tabulation of t expressions, above).

The resulting expressions for the prediction of the overall number of transfer units are:
For liquid-phase controlled systems

$$N_{tf_o} \approx N_{tb} + N_{tf} \tag{27}$$

$$N_{tb} = \beta_b\left[1 - \left(\frac{61.44}{75.72 + \mathcal{L}_f^{2.02}}\right)\exp\left(-\beta_1\frac{a_f^2}{\mathcal{L}_f\bar{\lambda}_b}\right)\right] \tag{28}$$

where

$$\bar{\lambda}_b = \lambda_{tf} = \lambda_t - \lambda_{\Delta f_o} + \lambda_{\Delta f} \tag{29}$$

$$\beta_b = \text{const} = 17.96\,\frac{\rho_L}{M_W}\exp\left[-\frac{(\sigma-\sigma_s)\omega}{R'T}\right] \tag{30}$$

$$\beta_1 = \text{const} = 0.526\,D_L V_b \tag{31}$$

$$\lambda_{\Delta f} = (\alpha_1\mathcal{L}_{1f} - \alpha_2\mathcal{L}_{2f})\left[\left(\alpha_1\frac{V_f}{V_{1f}}\right)\left(\frac{\lambda_\Delta}{\mathcal{L}}\right)_{1f} - \left(\alpha_2\frac{V_f}{V_{2f}}\right)\left(\frac{\lambda_\Delta}{\mathcal{L}}\right)_{2f}\right] \tag{46, 47}$$

$$\alpha_1 = \frac{l_f + 2l_{1f} + l_{2f}}{l_{1f} + l_{2f}}, \quad \alpha_2 = \frac{l_f + l_{1f}}{l_{1f} + l_{2f}} \tag{32}$$

$$N_{tf,1f,2f}^{(a')} = \beta\,\frac{a\mathcal{L}^{0.01}\lambda_\Delta}{\lambda_{tf,1f,2f}}\left[1 - 0.811\exp\left(-\beta_2\frac{a}{\lambda_\Delta\mathcal{L}^{1.01}}\right)\right] \tag{33}$$

where $N_t^{(a')}$ has been obtained by taking $l' = a'$ (see above tabulation of expressions for t):

$$\beta = 0.398\,\frac{V}{(S_B S_t)^{0.5}}\exp\left[-\frac{(\sigma-\sigma_s)\omega}{R'T}\right] = \text{const} \tag{34}$$

$$\beta_2 = 6.192\left(\frac{\rho_L D_L}{M_W}\right)S_B = \text{const} \tag{35}$$

$$N_{tf,1f,2f}^{(z)} = \frac{\beta'\lambda_\Delta}{\lambda_{tf,1f,2f}}\left[1 - 0.811\exp\left(-\beta_2\frac{a^2}{\mathcal{L}\lambda_\Delta}\right)\right] \tag{36}$$

where $N_t^{(z)}$ has been obtained by taking $l' = Z$ (see above, tabulation of expressions for t):

$$\beta' = \frac{V}{ZS_B}\exp\left[-\frac{(\sigma-\sigma_s)\omega}{R'T}\right] = \text{const} \tag{37}$$

$$\beta_3 = 2.465\,(S_B Z)\left(\frac{\rho_L D_L}{M_W}\right) = \text{const} \tag{38}$$

For gas-phase controlled systems

$$N_{tf_o} = N_{tp} + N_{tb} + N_{tf} \tag{39}$$

$$N_{tp} = \mathcal{D}_p\,\frac{\lambda_t}{G_v^{0.5}} \tag{40}$$

where

$$\mathcal{D}_p = \text{const} = 8.56\times 10^3\left(\frac{D_G P}{R^2T}\right)^{0.5}\left(\frac{M_W\mu_L}{g\rho_L^2}\right)^{0.167}$$

$$\frac{N_\lambda^{0.5}}{(b\sin\phi)^{0.167}}\exp\left[-\frac{(\sigma-\sigma_s)\omega}{R'T}\right] \tag{41}$$

$$N_{tb} = \mathcal{D}_b\,\frac{a_f}{G_v}\left(\frac{\bar{\lambda}_b}{\mathcal{L}_f}\right)^{0.5} \tag{42}$$

where $\bar{\lambda}_b$ is given by Equations (29) and (32) above:

$$\mathcal{D}_b = 81.63\,\frac{P}{RT}\left(\frac{M_W D_G}{\rho_L}\right)\frac{V_b}{(pS)^{0.5}}\exp\left[-\frac{(\sigma-\sigma_s)\omega}{R'T}\right] = \text{const} \tag{43}$$

$$N_{tf,1f,2f} = \mathcal{D}\,\frac{a}{G_v}\left(\frac{\bar{\lambda}}{\mathcal{L}}\right)^{0.5} \tag{44}$$

where $\bar{\lambda}$ is an arithmetic average of the incoming and outgoing flow rates:

$$\mathcal{D} = 57.72\,\frac{P}{RT}\left(\frac{M_W D_G}{\rho_L}\right)^{0.5}\frac{V}{(1'S)^{0.5}}\exp\left[-\frac{(\sigma-\sigma_s)\omega}{R'T}\right] = \text{const} \tag{45}$$

with l' taken equal to l
Finally

$$(N_t)_{\text{apparatus}} = N_{tp} + N_{tb} + N_{tf} + N_{t1f} + N_{t2f} \tag{46}$$

All the prediction expressions outlined above are usable if sufficient knowledge is available on the characteristics of flowing foams (say $\mathcal{L}$, a, λ_Δ, $\frac{v_H}{u_{\mathcal{H}}}$ as a function of λ_t, G_v, $l_1, \ldots_n$). This information has been obtained in preparation to the present work and is reported elsewhere (*46*, *47*).

RESULTS AND DISCUSSION

It has been shown that there exists an interrelationship between the basic flow and position parameters, with their dependent foam flow characteristics, and the prediction expressions for rates of desorption. This determines the change properties of, say N_t, as a function of either the liquid flow rate entering the apparatus† or the gas flow rate.

† It might be worth re-emphasizing that, in the case of flowing foams, there is a distinct difference between the liquid flow rate entering the apparatus and the successively decreasing liquid flow rates entering any arbitrary foam stage in a downstream direction, due to foam drainage.

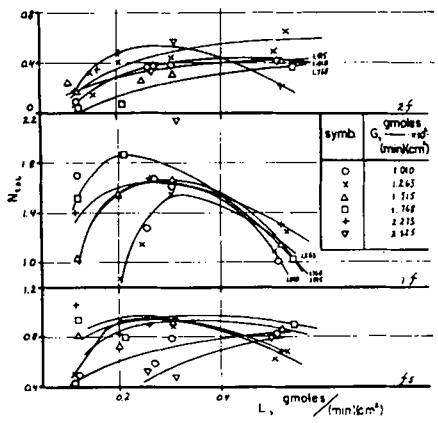

Fig. 4. N_{tol} vs. the liquid flow rate entering the apparatus, parameter: G, 1/16-in. perforations.

* N_{tf} cannot be added to the sum as it is based on a different liquid flow rate. At any rate, it assumes negligible values (for a contact length taken as $\frac{z_p A'_\sigma}{A'_p}$).

If one plots N_t vs. either of these two flow variables, a set of exponential curves is obtained that exhibits maxima in many instances.* This holds true for both liquid- and gas-phase controlled systems and for any position within the apparatus, and is illustrated in Figure 4 chosen from the many available sets of data (*46*).†

A few experimental results showing actual concentrations measured at various points within the apparatus are tabulated below in order to exemplify some typical separation performances:

System: CO_2-H_2O (0.2% Saponin)

d_h, in.	L, g. moles / (min.) (sq. cm.)	G, g. moles / (min.) (sq. cm.) $\times 10^2$	X_1	X_2 moles CO_2 / mole water $\times 10^4$	X_3	X_4
1/16	0.204	1.26	3.805	1.486	0.620	0.539
1/8	0.307	4.04	3.689	1.747	0.571	0.343

System: NH_3-H_2O (0.2% Saponin)

d_h, in.	L, g. moles / (min.) (sq. cm.)	G, g. moles / (min.) (sq. cm.) $\times 10^2$	Y_1*	Y_2*	Y_3*	Y_4*
			mm. Hg			
1/16	0.205	1.52	2.537	2.396	2.236	2.223
1/8	0.299	4.04	2.429	2.281	2.114	2.060

The predicted rates of mass transfer are compared with the experimental values in Figure 5.

The agreement in the case of ammonia desorption is good except at the low end of the range of gas and liquid flow rates. At this extreme the characteristics of moving foams might change drastically before a complete decay occurs. This would account for the lack of agreement.

For carbon dioxide desorption the experimental values tend to fall between the low (based on contact length = Z) and the high (based on contact length = a') predictions in the case of the active first foam stage. Only the low predictions are of any consequence for the inactive second foam stage, and the increased scatter is probably due to the higher experimental inaccuracy (very low concentrations to be measured).

The complexity of processes occurring in the foaming stage is also evident from the figure. Here, the experimental results range from lower than the lowest predicted values (at the critical end of flow rates range below which the foam decays rapidly) to higher than the highest predicted values [at the other end of the range, where the hydrodynamic regime is highly intensified and increased gas channeling contributes to more mixing in the liquid phase (*46, 47*)]. It is felt that at least part of the blame is to be laid on the difficulty of accurate assessment of interfacial areas in the foaming stage (*46, 47*) and on the nature of assumptions used for the physical model and the integration of the individual zone predictions into an overall figure for the stage.

The mass transfer performance in any stage of the apparatus, for a given flow rate, will depend also on the types of plate perforations (geometry), in line with what was reported on the characteristics of flowing foams (*46, 47*).

If the gas velocities through the plate perforations are about equal, that is if the superficial gas velocities in the duct stand in a ratio of about 1:4 (in this case), similar numbers of transfer units are obtained at the foaming stage, particularly for ammonia desorption. This is to be expected, since the mechanism of mass transfer in essentially gas-phase controlled systems will depend directly on the gas velocity (which determines the penetration time). Also, at least two of the three zones of the foaming stage, namely the plate and bubble formation zones, will perform according to the gas velocity through the perforations rather than through the duct.

For carbon dioxide desorption, where the agreement is less good, the dependence on gas flow rate can only be indirect, that is in terms of the flow characteristics of the bubble formation zone (drainage, interfacial areas, etc.).

* Here and in what follows it should be noted that correlations and presentation of results vs. a liquid-to-gas flow rate ratio were not found applicable. This, too, is due to the peculiar flow characteristics of aqueous and continuously draining foams. These can be markedly different at low and at high liquid and gas flows with the result that identical L/G values are related to different mass transfer data depending on the absolute magnitudes of the flow rates in question.

† Tabular material has been deposited as document 8252 with the American Documentation Institute, Photoduplication Service, Library of Congress, Washington 25, D. C., and may be obtained for $1.25 for photoprints or $1.25 for 35-mm. microfilm.

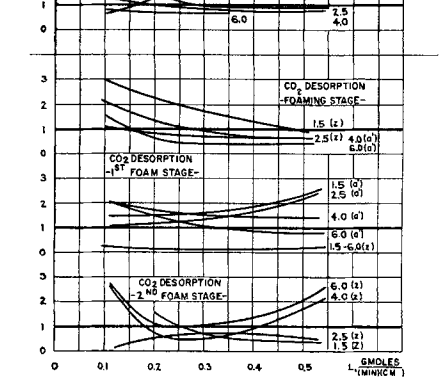

Fig. 5. Graphical representation of prediction accuracy-Parameter: G, g. moles / (min.)(sq. cm.) $\times 10^2$ (in brackets: contact length on which N_{tpr} is based).

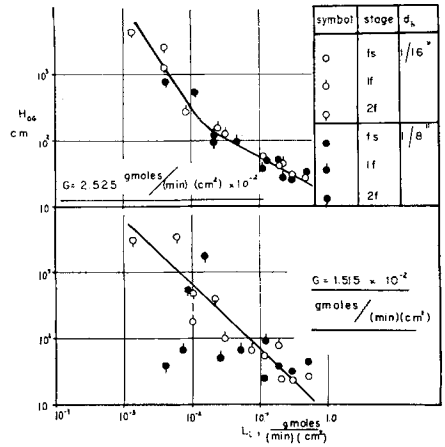

Fig. 6. H_{OG} vs. the liquid flow rate entering any stage, Parameter: G.

Considering now the relationship between the overall height of a transfer unit (rather than the number of transfer units) and the liquid flow rate entering any given stage (rather than the apparatus), one observes a log-log type of correlation trend particularly for the case of ammonia desorption. This is illustrated in Figure 6. Although this fact is interesting, the prediction equations that have been developed based on the liquid flow rate entering the apparatus (and thus easy to determine and control) have a more practical significance. One notices that at higher gas flow rates differences in the plate geometry are no longer evident, and the scatter of the data is much reduced. Conversely, a break point appears at $L_i \approx 2 \times 10^{-2}$ g.moles/(min.)(sq.cm.) (the same value also in the case of carbon dioxide desorption). Below this flow rate a higher rate of increase of H_{OG} with decrease in L_i is obtained which is to be expected, since:

$$\lim_{L_i \to O} H_{OG} = \infty$$

Figure 7 indicates a straight-line correlatibility between bulk viscosity or surface tension and the carbon dioxide desorption performance. These two physical parameters are important factors in any foaming system (*46, 47*).* An increase in surface tension brings about an increase in the rate of transfer (particularly for the first foam stage, which also has the main transfer role). The undesirable fact that for a higher surface tension foams are less stable and the corresponding starting solutions are less foamable is more than offset by the following factors:

1. Small resistance to diffusion since the surfactant-determined interfacial resistance term is exponentially dependent on the surface tension gradient between a solution and the same solution with surfactant added to it. Thus, a higher surface tension of the foaming solution (that is less surfactant) decreases the gradient and, with it, the magnitude of the interfacial resistance term.
2. The drainage rates from any given stage increase with an increase in surface tension (*46, 47*); this leads to shorter liquid-gas contact times and higher rates of desorption.
3. The resulting lower foam stability is conducive to a more intensified process of decay with more foam bubbles bursting in a given volume of the duct. More mixing or a shorter gas-liquid contact length is the result with the same consequence as above.

In conclusion, the limit to higher mass transfer rates appears to be the highest surface tension, that is lowest concentration of surfactant, at which a solution will produce a flowing foam. In the present case this limit has been attained at $\sigma \approx 45$ dynes/cm., corresponding to approximately 0.1% Saponin by weight.

An exactly opposite effect is obtained when the bulk viscosity of the solution increases for the reasons outlined in points 2 and 3 above.

* See second footnote on page 360.

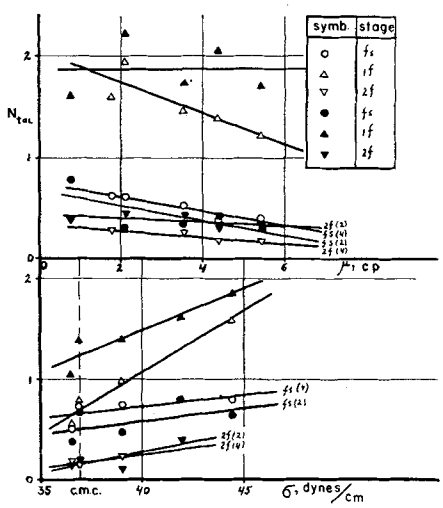

Fig. 7. Influence of the physical properties of the foaming solution on N_{tol} (1/16-in. perforations) (clear points—2.02 × 10^{-2} g.moles air/(min.)(sq. cm.), 0.316 g.moles water/(min.)(sq. cm.), black points—1.01 × 10^{-2} g.moles air/(min.)(sq. cm), 0.312 g.moles water/(min.)(sq. cm).

COMPARISON WITH OTHER DATA

A direct comparison with other types of equipment utilizing foams or froths, or conventional hardware such as packing is made difficult by the following reasons:

1. The data reported in the literature for foam, froth, or gas-bubble columns refer to countercurrent operation at flow rates considerably in excess of those used in the present work. Such relatively high flow rates would be unpractical anyway, owing to foam decay problems in this case.
2. The present paper deals with the rather unusual situation of a decreasing liquid flow rate (as a function of the position in the apparatus) caused by foam drainage. The data available for comparison are all, of course, reported for a constant liquid flow rate.

Figure 8 compares some data in terms of the overall height of a transfer unit based on the liquid phase vs. the air flow rate. The considerable discrepancy in liquid flow rates is obvious, although use has been made only of the data that were obtained in the present work at the highest liquid flow rates. It is apparent that the other data for H_{OL} are higher with some exceptions in the case of the inactive second foam stage.

CONCLUSIONS

1. It has been shown that a workable mass transfer device can be operated, based on a horizontal column of a stable aqueous foam in motion. This foam can readily be generated over a certain range of gas-liquid flow rate combinations, and its formation and existence are the result of an induced surface activity in the liquid phase (by addition of 0.2% by weight of Saponin). There are no energy requirements other than those necessary for the flow of gas through a perforated plate, where the foam is produced, and through the empty duct that is to be filled by the moving foam.

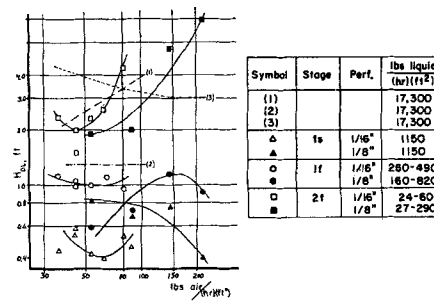

Fig. 8. Comparison with other data. (1)— Reference 21—adsorption of carbon-dioxide by surfactant-treated water, porous plate columns. (2)—Reference 40—desorption of carbon-dioxide from water in gas bubble columns (porous plate)—extrapolated curve. (3)—Cooper, C. M., et al., *Trans. Am. Inst. Chem. Engrs.*, 37, 979 (1941)—same liquid flow rate as (1); adsorption of carbon dioxide by water; packed column with 2-in. Raschig rings—interpolated data.

2. After a certain length of travel in the downstream direction, during which the foam films are continually losing their liquid content by drainage, a foam becomes inactive with resulting low drainage rates and separation efficiencies.

3. At a given gas flow rate, different foam flow behavior results for different plate geometries. In this case this refers to a ratio of nearly 1:4 in the percent free area. In turn, differences are caused in the mass transfer performance. The only cases where some similarities are observed correspond to equal gas velocities based on the plate free area at the foaming stage. These similarities are apparently due mainly to the plate and bubble formation zones that are expected to be susceptible to the gas velocity through the perforations rather than to the superficial gas velocity in the duct. Indeed, a higher degree of similarity in performance is obtained for ammonia desorption, where the dependence on the gas flow is direct (as per the prediction theory outlined in this paper) rather than in terms of foam characteristics, as for carbon dioxide desorption.

4. The mass transfer performance of stable foams in movement becomes better as their foamability and foam stability decrease. This situation corresponds to an increase in surface tension (for a betterment in performance) and continues up to the point beyond which no more moving foam can be generated.

This characteristic may be approximated by a linear relationship between σ and N_{toL}. It is explainable on the basis of the analytical model for predictions of mass transfer rates and in terms of the foam flow correlations reported elsewhere (*46, 47*).

5. The mass transfer performance of stable foams in movement becomes poorer as the bulk viscosity of the foaming solution increases, and this change can also be described by a linear correlation and explained as for point 4 above.

6. Some types of foam equipment, all of them based on countercurrent contacting in vertical towers, have already been studied and their efficiencies and/or rates of mass transfer found generally superior to those of conventional types of hardware (packed towers, for instance).

The moving foam systems studied in the present work exhibit sometimes similar but generally significantly better mass transfer performances when compared with the other types of foam equipment, while operating at much lower liquid flow rates (one order of magnitude or more) and lower gas flow rates. This, and also the negligible pressure drop ascribable to the interaction of the gas and liquid streams, should compensate for the disadvantage of larger volumes of equipment per unit flow rate (as compared with countercurrent tower operation).

7. The various parameters and criteria for a moving foam interact in such a way that if one expresses the performance (say N_t or η) as a function of liquid flow rate or of gas flow rate only, a maximum is exhibited in many instances.

8. The height of a transfer unit appears to be correlatable exponentially, with a certain degree of scatter, in terms of the incoming liquid flow rate to any foam stage (at any longitudinal position in the duct). This is particularly the case for gas-phase controlled systems and higher gas flow rates. Thus, an alternative way of defining mass transfer performances would be available. However, it is believed that a definition based on the liquid flow rate entering the apparatus is more practical from the standpoint of its applicability to predictions.

Below a given value of incoming liquid flow rate, identical for the cases of ammonia and carbon dioxide desorption (because their foam flow behavior is identical), the curve of H_{oL} or H_{oG} vs. L_i exhibits a break. This break characterizes a certain stage of foam decay that has been reached, beyond which rapid deterioration occurs in the mass transfer performance with, at the limit, $H_{oL} = H_{oG} = \infty$ (for $Li = 0$).

9. An analysis of the hydrodynamics of moving foams and of the mass transfer occurring in them is possible by means of a distinct definition of a foaming stage, where the foam is generated, and of several foam stages of an arbitrary length, composing the moving foam column. The foaming stage, in turn, is definable as a composite of several distinct zones, each one with its specific performance and behavior: the plate zone, where the foam generation is started by cross current gas-liquid interaction; the bubble formation zone, where bubbles are formed, grow, and and coalesce into a stable, true, foam; and the foam zone, which is the upstream end of the moving foam column.

10. The mass transfer performance of moving stable aqueous foams can be defined and predicted, for both a liquid- and a gas-phase controlled system, in terms of three basic parameters: gas flow rate, liquid flow rate entering the apparatus, and longitudinal position in the duct. These parameters act interdependently either directly, as an independent variable, or indirectly, in terms of the characteristic foam criteria: fractional liquid holdup, interfacial area, drainage flowrate, gas channeling.

The predictions are based on a model of crosscurrent interaction between the phases whether within the moving foam or at the foam source (where it is generated), and on several correction factors: An interfacial resistance term of a physico-chemical nature, due to the presence of surfactant in the solution, a term accounting for the finiteness of the liquid medium in which transfer occurs, and, a term accounting for the gas channeling effects in the moving foam column.

ACKNOWLEDGMENT

The authors gratefully acknowledge financial support of this work by the U.S. Public Health Service, Research Grant No. AP 00024-05.

NOTATION

A = area of mass transfer sq.cm.
A' = area of given geometry sq.cm.
a = interfacial area, sq.cm./cc. of given volume
a' = average foam cell (bubble) size, cm.
B = the slope, in linear correlation
b = width of rectangular duct, cm.
D = diffusivity, sq.cm./sec.
d_h = diameter of plate perforation, cm.
$\mathcal{D}$ = constant in Equations (40) to (45)
F = intercept, in linear correlation
G = molar gas flow rate, g.moles/(min.)(sq.cm. duct cross section)
G_v = standard volumetric gas flow rate, std. cu.ft./min.
g = acceleration of gravity = 980.1 cm./sec.^{2}
H = height of a transfer unit, cm.
K_G = overall mass transfer coefficient based on a driving force in g.moles/cc., cm./sec.
L = molar liquid flow rate entering the apparatus = sum of measured outflowing liquid streams, g.moles/(min.) (sq.cm. duct cross section)
l = (horizontal) length of given stage, cm.
l' = characteristic gas-liquid contact length, in any direction, cm.
$l_{1,\ldots,n}$ = longitudinal coordinate, cm.
$\mathcal{L}$ = fractional liquid holdup, cc./cc. apparatus section
M = molecular weight
M_t = amount of component transferred per unit area in time t, g.moles
M_∞ = amount of component transferred per unit area in time $t = \infty$, g.moles
N = rate of mass transfer, g.moles/sec.

N_h = number of plate perforations
N_t = number of transfer units
P = ambient pressure, mm.Hg
p = pitch of perforated plate, cm.
R = gas constant = 62,363.3 (mm.Hg)(cc.)/(g.mole)(°K.)
R' = Boltzmann constant = 1.3804×10^{-16} erg./(°K.)(molecule)
r_i = internal radius of hollow sphere, cm.
r^2 = square of the correlation coefficient
S = cross-sectional duct area (perpendicular to horizontal direction of flow, sq.cm.)
S_B = cross section parallel to bottom of duct, sq.cm.
S_l = cross section parallel to lateral duct sides, sq.cm.
$s_{y|x}$ = standard error of the estimate (7)
T = absolute temperature, °K.
t = penetration time, sec.
u = gas velocity (in general), cm./sec.
V = volume of given apparatus section, cc.
v = liquid velocity (in general), cm./sec.
X = liquid-phase concentration, moles/mole water
Y = gas-phase concentration, moles/mole air
Z = height of duct, cm.
z = travel distance of downflowing liquid, cm.

Greek Letters

$\alpha_1 = \dfrac{l_f + 2l_{lf} + l_{sf}}{l_{lf} + l_{sf}}$, $\alpha_2 = \dfrac{l_f + l_{lf}}{l_{lf} + l_{sf}}$

β, β', etc. = constants in Equations (30), (31), (34), (35), (37), (38)
γ = molar gas flow rate, g.moles/sec.
δ' = average thickness of foam cell film (lamella), cm.
η = stage efficiency defined as $(X_i - X_o)/(X_i - X_o^*)$ or $(Y_o - Y_i)/(Y_o^* - Y_i)$, fraction of unity
λ = molar liquid flow rate, g.moles/sec.
μ = viscosity, poises
ρ = density, g./cc.
σ = surface tension, dynes/cm.
ϕ = angle of plate with respect to horizontal, deg.
ω = area of solute molecule at the interface, sq. cm.

Subscripts

A = air
app = apparatus
b = bubble formation zone
ex = experimental
f = foam zone
fs = foaming stage
$1f$ = first foam stage
$2f$ = second foam stage
G = gas phase
H = in a horizontal direction
$\mathcal{H}$ = based on the fractional gas holdup
i = incoming flow or concentration to any defined section of the apparatus (note: i used alone indicates inlet to the apparatus as a whole, that is to the plate zone) (λ_i)
L = liquid phase
OG = overall, based on the gas phase
OL = overall, based on the liquid phase
o = outgoing flow or concentration from any defined section of the apparatus
p = plate zone
pr = predicted
W = water
Δ = draining out
σ = based on the plate free area
ϕ = based on a finite medium
Σ = based on a semi-infinite medium

Superscripts

(bar) = average
* = equilibrium (interface)

LITERATURE CITED

1. Anderes, G., Ph.D. thesis, No. 3101, Zurich, Switzerland (1961).
2. ———, *Chem. Ing. Tech.*, **34**, 597-602 (1962).
3. *ASTM Test No. D1173-53*, adopted 1954.
4. *ASTM Standard D1331-56*, adopted 1956.
5. Calderbank, P. H., and M. B. Moo-Young, *Chem. Eng. Sci.*, **16**, 39-54 (1961).
6. Calvert, S., and G. Kapo, *Chem. Eng.*, **70**, 99-104 (February, 1963); also *ibid.*, 105-110 (March, 1963).
6bis. Crank, J., "The Mathematics of Diffusion," Oxford at ruary, 1963); also *ibid.*, 105-110 (March, 1963).
7. Crow, E. L., et al., "Statistics Manual," pp. 156 et seq., Dover Publications, New York (1960).
8. Drouhin, R., *Génie Chim.*, **85**, 23-29 (1961).
9. Defay, R., and I. Prigogine, "Surface Tension and Adsorption," vol. 2 of the Treatise of Thermodynamics, in French ed., Desoer, Liège, Belgium (1951).
10. Drozdov, N. P., et al., *J. Appl. Chem.* (*USSR*), **33**, 2572-2575 (1960).
11. Fesenmeyer, H., Ph.D. thesis, No. 3066, Zurich, Switzerland (1960).
12. Grassmann, P., and G. Anderes, *Chem. Ing. Tech.*, **31**, 154-155 (1959).
13. Helsby, F. W., and D. C. P. Birt, *J. Appl. Chem.* (*London*), **5**, 347-352 (1955).
14. Higbie, Ralph, *Trans. Am. Inst. Chem. Engrs.*, **31**, 365-389 (1935).
15. Houghton, G., et al., *Chem. Eng. Sci.*, **7**, 26-39 (1957).
16. Johnson, A. I., and C. W. Bowman, *Can. J. Chem. Eng.*, **36**, 253-261 (1958).
17. Kadlas, P., and S. Veseley, *Chem. Prumysl.*, **10**, 565-571 (1960).
18. Kuzminykh, I. N., *Khim Prom.*, 234-237 (1956).
19. ———, and A. I. Rodionov, *J. Appl. Chem.* (*USSR*), **29**, 1433-1438 (1956).
20. *Ibid.*, **32**, 1523-1528 (1959).
21. Metzner, A. B., and L. F. Brown, *Ind. Eng. Chem.*, **48**, 2040-2045 (1946).
22. Mochalova, L. A., and M. K. Kishinevsky, *J. Appl. Chem.* (*USSR*), **28**, 25-33 (1955).
23. *Ibid.*, **29**, 193-198 (1956).
24. *Ibid.*, **31**, 525-533 (1958).
25. *Ibid.*, 1007-1012.
26. Mukhlenov, I. P., *ibid.*, 1328-1333.
27. ———, and E. S. Tumarkina, *ibid.*, 1635-1642.
28. Mutzenberg, A., *Chem. Ing. Tech.*, **34**, 542-546 (1962).
29. Poll, A., and W. Smith, *Trans. Inst. Chem. Engrs.*, **40**, A93-A97 (1962).
30. Pozin, M. E., *J. Appl. Chem.* (*USSR*), **25**, 1097-1105 (1952).
31. ———, and B. A. Kopylev, *ibid.*, **30**, 383-389 (1957).
32. *Ibid.*, **31**, 375-380 (1958).
33. Pozin, M. E., and E. Y. Tarat, *ibid.*, 1318-1327.
34. Pozin, M. E., et al., *ibid.*, 838-846.
35. *Ibid.*, **32**, 1027-1032 (1959).
36. *Ibid.*, pp. 1033-1038.
37. Ross, J., and G. D. Miles, *Oil and Soap*, **18**, 99-102 (May, 1941).
38. Ross, J., et al., *U. S. Pat. 2,315,983* (Apr. 6, 1943).
39. Ruckenstein, E., *Rev. Chim.* (*Bucharest*), **12**, 97-98 (1961).
40. Shulman, H. L., and M. C. Molstad, *Ind. Eng. Chem.*, **42**, 1058-1070 (1950).
41. Tarat, E. Y., *J. Appl. Chem.* (*USSR*), **34**, 1846-1851 (1961).
42. ———, and S. A. Bogatykh, *ibid.*, 1788-1791.
43. Ungemach, M., *Chem. Ing. Tech.*, **33**, 632 (1961).
44. Vignes, A., *J. Chim. Phys.*, **57**, 999-1005 (1960).
45. Vlcek, V., et al., *Intl. Chem. Eng.*, **2**, 216-220 (1962).
46. Weissman, E. Y., Ph.D. thesis, Case Institute of Technology, Cleveland, Ohio (1963).
47. ———, and S. Calvert, to be published.
48. Workman, W. L., Ph.D. thesis, Case Institute of Technology, Cleveland, Ohio (1963).

Manuscript received March 16, 1964; revision received November 4, 1964; paper accepted November 18, 1964. Paper presented at A.I.Ch.E. Pittsburgh meeting.